

Impact of tailings dam failure on spatial features of copper contamination (Mazraeh mine area, Iran)

Amir Khamseh¹ · Farzin Shahbazi¹ · Shahin Oustan¹ · Nosrattollah Najafi¹ · Nasser Davatgar²

Received: 9 January 2017 / Accepted: 19 May 2017 / Published online: 2 June 2017
© Saudi Society for Geosciences 2017

Abstract Mining activities pose a potential risk of metal contamination around mining sites. On May 6, 2010, a tailings dam failure of the Mazraeh copper mine near Ahar in East Azerbaijan province, Iran, released vast amounts of mine wastes. To better understand the magnitude of copper contamination in the waste-affected soils, it is important to assess the spatial distribution of soil copper content at unsampled points. A total of 30 soil samples and their surficial sediments together with the 6 uncontaminated control samples (0–10 and 10–30 cm) were collected along the stream flow that joined Ahar-Chai River. Some of soil properties as well as total copper concentration were determined in all samples. The mean value of the latter in the surface contaminated soils was found to be approximately two times more than controls. Furthermore, the mean concentration of copper in the surface loaded material was 10 times more than the soils. High copper concentrations were observed in surficial sediments of the soils near the broken tailings dam. The Inverse Distance Weighting (IDW) method was employed in data analysis. The spherical and Gaussian semivariogram models were properly fitted to the data of copper contents in soils and surficial sediments.

Keywords Ahar · Contamination · Copper mining · Iran · Spatial distribution · Tailings dam

This article is part of the Topical Collection on *Water Resource Management for Sustainable Development*

✉ Farzin Shahbazi
shahbazi@tabrizu.ac.ir

¹ Soil Science Department, Faculty of Agriculture, University of Tabriz, Tabriz 5166616471, Iran

² Soil and Water Research Institute of Iran, Karaj, Iran

Abbreviations

IDW	Inverse Distance Weighting
GPS	Global Positioning System
EC	Electrical conductivity
CEC	Cation exchange capacity
OC	Organic carbon
CCE	Calcium carbonate equivalent
CF	Contamination factor
SCC	Soil copper concentration
CCS	Copper concentration of surficial sediments
C_0	Nugget
C_0+C	Sill
A_0	Range of parameter
RSS	Residual sum of squares
DSM	Digital soil mapping
CV	Coefficient of variation
UTM	Universal Transfer Mercator

Introduction

Paying attention to contamination causes and sources and also to monitoring pathways is the main objectives in rational use of soil resources and environment. Increasing human activities during the last decades have induced widespread release of heavy metals in the environment. Industrial products, mines, transport, and even uncontrolled application of pesticides are the known sources to establish heavy metal contamination (Hutton and Meeus 2001). These metals may spread to the soil by sewage application, wastewater irrigation, and atmospheric deposition (Salomons 1992).

Late in the 1970s, pedologists realized the possible employment of geostatistics in soil survey. They also developed methods to make maps of individual soil properties without having to classify the soil and getting embroiled in all the

doubts and controversy (Webster 2008). Due to the impossibility of making the samples of all data points, geostatistical approaches were used to predict the spatial and temporal distribution of a variable and create maps as well. These provide descriptive tools such as semivariograms to characterize the spatial pattern of continuous and categorical soil attributes (Goovaerts 1999). A lead risk map for Wolverhampton, England, was provided using a spherical model and kriging interpolation method, in which near surface soil lead concentrations showed a degree of spatial correlation on a city scale (Hooker and Nathaniel 2006). A comparative study of interpolation methods for mapping soil properties revealed that the correlation coefficients between experimental data and estimated results of kriging were higher and its mean absolute errors were lower than those of Inverse Distance Weighting (IDW) method (Kravchenko and Bullock 1999). Nevertheless, the high accuracy of that method for studying of nitrogen distribution pattern has previously been reported (Gotway et al. 1996). This approach was also confirmed by others to predict the spatial distribution of heavy metals in floodplain soils around the Gule River in the Netherlands (Leenaers et al. 1990).

Climate change in Iran is likely to cause the conversion of agricultural lands into the marginal ones. As well known, the bioclimatic changes are out of our monitoring, whereas mining and manufacturing development should be perfectly controlled. Disturbance of mines, whose owners do not obey the laws of rehabilitation, is potentially detrimental to the environment (Shahbazi and De la Rosa 2010). Tailings dam are structures built to impound wastes from mining activities. Currently, thousands of tailings dam worldwide contain billions of tons of waste material at mining sites. Tailings dam should be constructed to achieve a stable and safe state. Unfortunately, since 1970, more than 35 tailings dam failures reported around the world. The Aznalcollar (Spain) and Sasa (Macedonia) accidents occurred in 1998 and 2003 caused an intensive flow of tailing materials through the rivers of Guadiamar and Kamenica, respectively (Vrhovnik et al. 2013). Copper is the main contaminant in the soils of copper mining areas of the world. Moreover, copper is an essential nutrient to all organisms but is toxic at high concentrations (Adriano 2001). Some of researchers have reported the spatial distribution of soil copper in relation to relevant soil properties (Grzebisz et al. 2001; Jafarnejadi et al. 2013; Sun et al. 2014).

The study site of this research work was around the Mazraeh copper mine which has been established since 1960 in the Northwest of Iran. The refining capacity of this refinery is expected to be 250 t copper per day. Copper ore concentration processes create wastes (tailings) that are directed to the ponds for storage. Therefore, the marginal agricultural areas are thought to be at risk of exposure to heavy metals, particularly copper. On May 6, 2010, after a heavy rain, the poor construction of the tailings dam caused to

collapse and then to discharge the effluent into a seasonal stream, namely Mazraeh-Chai, that empties into Ahar-Chai River. Because of low capacity of the stream channel, massive flooding and triggered mudslide occurred in the marginal lands. The tailings flow material comprised high concentrations of some heavy metals, particularly copper which may adversely affect the environment. Consequently, we investigated the patterns of copper spatial distribution in the vicinity of the failed dam. This study deals with the characteristics of the soils and their surficial sediments after the accident.

Materials and methods

Study area

This study was performed in an area of about 1500 ha located in the Mazraeh region of Ahar County in East Azarbaijan province, Iran (Fig. 1).

The area lies within the coordinates of longitude 47° 02' 47" to 47° 03' 46"E and latitude 38° 31' 56" to 38° 37' 12" N. There are cultivations, orchards, and voids along the pathway of seasonal stream. The geology of the study area belongs to quaternary period and characterized by high level piedmont fan and valley terraces deposits. The dominant soil orders in this region were classified as Inceptisols.

Sampling and preliminary analysis

Composite sampling was conducted at 30 sites close to the pathway of Mazra-Chai seasonal stream (Fig. 1) in May 2011 for determining the total concentration of copper not only at both upper (0–10 cm) and lower (10–30 cm) soil depths (indicated as surface and subsurface soils) but also at surface accumulated (surficial) sediments. The samples were collected on the line, spaced 300 m apart, from the tailings dam to about 10 km away where the effluent was being discharged and expanded through the marginal lands. Moreover, six control soil samples were collected some meters away from the contaminated area but not covered by sediment. Global Positioning System (GPS) was used to provide the geographical coordination of sample points.

Soil samples were air-dried and then sieved through a 2-mm mesh. Some common physical and chemical properties including texture (Gee and Bauder 1986), electrical conductivity (EC) (Rhoades 1996), pH (Thomas 1996), cation exchange capacity (CEC) (Chapman 1965), organic carbon (OC) (Nelson and Sommers 1982), and calcium carbonate equivalent (CCE) (USDA-SCS 2004) were determined. The soil copper concentration (SCC) at two depths and copper concentration of surficial sediments (CCS) were measured using aqua regia method (Chen and Ma 2001). Half a gram

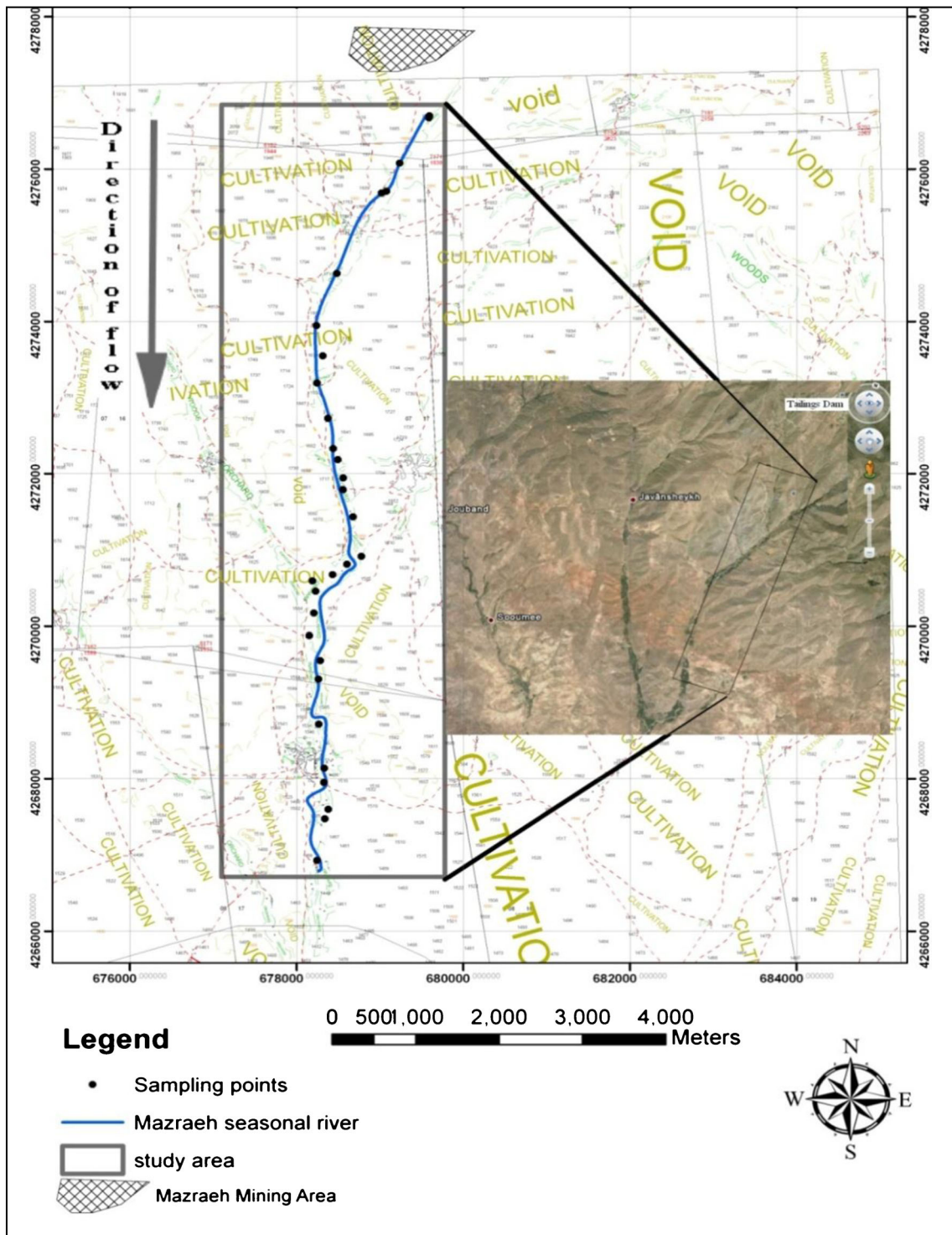


Fig. 1 Study area and sampling points setting

(0.5 g) of the soil or sediment sample was digested with 12 mL of aqua regia solution (HNO₃/HCl, 1:3 ratio) and allowed to stand overnight. Then, the sample was digested at 110 °C for 3 h. The digest was allowed to cool and filtered through Whatman no. 42 paper into a 100-mL standard volumetric flask. The filtrate was analysed for Cu using flame atomic

absorption spectrometry, “Shimadzu, 6300.” To evaluate the pollution status of soils before and after the accident, a contamination factor (CF) was calculated using the concentration of copper in each sample compared to its concentration in the control samples. It was also divided into four categories according to previous investigations (Hakanson 1980).

Statistical analysis

Statistical analysis was performed using the Statistical Package for Social Science (version 16.0; SPSS Inc., Chicago, IL, USA). Descriptive statistics of the selected soil and sediment properties, i.e. mean, minimum, maximum, standard deviation, coefficient of variability, skewness, and kurtosis, were calculated. For normality, the original dataset were tested by one-sample Kolmogorov-Smirnov approach (Webster 2001). The relationships between SCC and soil physical-chemical properties were found via Pearson correlations using Eq. (1). The correlation coefficient, r , measures the strength and direction of linear correlation. A value close to +1 or -1 signifies a strong relation; one close to zero signifies a weak one.

$$r = \frac{\frac{1}{N-1} \sum_{i=1}^N (Z_i - \bar{Z})(y_i - \bar{y})}{\sqrt{s_y^2 \times s_z^2}} \quad (1)$$

where S_y^2 and S_z^2 are the variances of y and z , as two measured variables, respectively.

Modelling the variogram

The geostatistical analysis was carried out by the software GS+ for the environmental sciences, version 5.1. The datasets were normalized to improve the results of the modelling. Three theoretical models including spherical, Gaussian, and exponential models were adjusted to the semivariograms. The degree of spatial dependence of a random variable $Z(x_i)$ over a certain distance was computed by the following semivariogram (Eq. 2).

$$\gamma(h) = \frac{1}{2N(h)} \sum [z(x_i) - z(x_{i+h})]^2 \quad (2)$$

where, $\gamma(h)$ is the semivariance for the interval distance class h , $N(h)$ is the number of pairs of the lag interval, $Z(x_i)$ is the measured sample value at point i , and $Z(x_{i+h})$ is the measured sample value at position $(i+h)$. Uniform intervals were defined as a lag class distance intervals. The parameters of the appropriate data model including nugget (C_0), sill (C_0+C), and range of parameter (A_0) were derived with higher R^2 and lower residual sum of squares (RSS). The nugget effect represents the undetectable experimental error and field variation within the minimum sampling space and the sill represents total spatial variations.

Spherical model

The spherical function provides the main features of bounded variogram models (Eq. 3).

$$\gamma(h) = c \left\{ \frac{3h}{2a} - \frac{1}{2} \left(\frac{h}{a} \right)^3 \right\} \text{ for } h \leq a \text{ and } \gamma(h) = c \text{ for } h > a \quad (3)$$

where c is the sill variance and a is the range.

Exponential model

The exponential function is defined by Eq. 4, where c is the sill as before and r is a distance parameter.

$$\gamma(h) = c \left\{ 1 - \exp\left(-\frac{h}{r}\right) \right\} \quad (4)$$

Gaussian model

Unlike the two above models which increase from their origins with decreasing gradient, some others (like Gaussian model) appear to increase in gradient from the origin and then curve with decreasing gradient (Eq. 5).

$$\gamma(h) = c \left\{ 1 - \exp\left(-\frac{h^\alpha}{r^\alpha}\right) \right\} \quad (5)$$

where c and r have the same meaning as in the exponential model and α is an additional parameter, with $1 < \alpha \leq 2$. Clearly, if $\alpha=1$, then the model is exponential. However, α value greater than 1 creates reverse curvature near the origin. The limiting $\alpha=2$ defines the so-called Gaussian model.

Fitting the model

There are practical considerations determining the best approach to use in any given circumstance (Henderson et al. 2008). The method of IDW was used to spatial interpolation of all variables in the study area (Lark and Ferguson 2004). The models were fitted based on fundamental hypothesis of the IDW method which assumes that each measured point has a local influence that diminishes with distance. The Geostatistical Analyst Wizard tool was used to digitize the map of the study area. Both IDW and kriging methods are most widely used interpolation tools, but the IDW method was chosen due to limited data (i.e. <50 data points), poor distribution of these across the study area, and simplicity (Elliot et al. 2000). The IDW approach is based on the

assumption that the attribute value of an unsampled point is the weighted average of known values within the neighbourhood, and the weights are inversely related to the distances between the prediction location and the sampled locations (Whelan et al. 1996). There are different kinds of IDW according to its power as well as our objective does not meet to apply all of them. Either isotropy hypothesis or IDW² was also conducted in this research work.

Spatial interpolation and its uncertainty will be used by automated anisotropic Inverse Distance Weighting Cross-Validation/Jackknife approach (Tipper 2008). In cross-validation, each measured point is removed and compared to the predicted value for that location (Lu and Wong 2008). It is suggested to have field observations to verify the model outputs by adding the coordinate of tested samples on digital maps which is missing in this article.

Geographic information system

Geographic information system (GIS) is a computer-based system which provides data capturing and preparation, data management, manipulation, and presentation. Spatial or georeferenced data can be produced by GIS thematic maps. Therefore, production, dissemination, and use of maps play an

important role in cartography. The maps created represent certain levels of detail, which is dependent on the scale. One cannot only compare the results but also offer recommendations for point to point of the study area.

Finally, the data file was transferred to a congenial program, i.e. ArcGIS 10.1, a popular package with excellent graphics. ArcMap as a main application in ArcGIS was used for all mapping and editing tasks in the present study. The area of each mapping unit was then calculated to find the spatial variability of the copper contamination in the field scale. In a digital soil mapping (DSM) project, for example, the soil biological indices have been mapped using a regression-kriging method (Shahbazi et al. 2013).

Results and discussion

Data descriptions and statistical analysis

The statistical descriptive analysis of data is summarized in (Table 1). The high and low values of coefficient of variation (CV) belong to OC content and pH, respectively. All parameters except OC (both depths), SCC, and CEC (0–10 cm depth) had normal distributions. Logarithmic conversion was used to normalize their distributions. The normalized data of OC, SCC, and

Table 1 Descriptive statistics for selected properties of the surficial sediments and the investigated soils at two depths (no 30)

Soil properties	Depth (cm)	Mean	Min.	Max.	SD	CV (%)	Skewness	Kurtosis
Sand (%)	0–10	53.8	22.1	83.5	12.3	22.8	0.1	1
	10–30	57.7	40.6	80.6	11.2	19.4	0.3	1
Silt (%)	0–10	32.4	8.7	50.8	9	27.7	0.3	0.6
	10–30	28.7	13.9	47.9	9	31.2	0.3	0.4
Clay (%)	0–10	13.8	6	27.1	5.6	40.4	0.6	0.5
	10–30	13.6	5.5	24.7	5.9	43.3	0.5	1.1
CCE (%)	0–10	5.3	0	13.8	3.4	64.2	0.5	0.15
	10–30	4.5	0	10.1	2.57	57.1	0.1	0.3
pH	0–10	8.1	8.4	7.7	0.2	2	0.5	0.3
	10–30	8.3	7.6	8.6	0.2	2.4	1.4	2.6
EC (dSm ⁻¹)	0–10	1.09	0.37	2.67	0.5	42.2	1.4	3.4
	10–30	0.9	0.5	2.1	0.4	43.9	1.8	3.3
OC (%)	0–10	1.92	0	13.16	2.3	118.7	4.3	21.9
	10–30	1.4	0	12.3	2.1	149.3	4.9	25.8
CEC (cmol _c kg ⁻¹)	0–10	26	15.8	54.8	6.9	26.4	2.5	10.1
	10–30	23.2	12.7	36.7	5.6	30.7	0.3	0.02
SCC (mg kg ⁻¹)	0–10	105.3	72.6	257.9	34.4	32.6	3.2	13.5
	10–30	86.4	59.2	154.3	18.2	21.1	1.7	5.6
CCS (mg kg ⁻¹)	-----	1288	444	1854	289	23.2	0.7	1.4

SD standard deviation, CV coefficient of variations, CCE carbonate calcium equivalent, pH soil reaction, EC electrical conductivity, OC organic carbon, CEC cation exchange capacity, SCC soil copper concentration, CCS copper concentration of surficial sediments

CEC were back transformed to the original scale in DSM. The analysis of geochemical mobility for the tailings of Sarcheshmeh mine showed that copper had the highest mobility among the heavy metals present (Khorasanipour and Eslami 2014). A point by point observation of total copper concentrations for soils and surficial sediments of the study area are fully presented in a Universal Transfer Mercator (UTM) coordinate system (Table 2). The values of CF in each sampling point at two depths are also presented. The mean total concentration of copper at upper 10 and 10–30 cm depth of the control soils were 49.7 and 48.8 mg kg⁻¹, respectively. These values were used to calculate the contamination factors of copper for the contaminated soils. The mean total concentration of copper at upper 10 cm, 10–30 cm, and surficial sediments was 105.3, 86.4, and 1116 mg kg⁻¹, re-

spectively. The guideline values for copper were established for soils at different textures as follow (in mg Cu kg⁻¹): clay, 100; loam, 60; and sand, 30 (Kabata-Pendias 2011).

Considering the dominance of sandy loam and loam soil textures in the study area, one can use the guideline value of 60 mg kg⁻¹. Therefore, the mean total concentration of copper in upper and lower soil depths was approximately 1.75 and 1.44 times higher than the guideline value. However, the copper content of the control soils is lower than the guideline value. Much higher concentrations of copper (1900 and 925 mg kg⁻¹) were respectively reported in paddy soils of China, around the Dexing Copper Mine, in Jiangxi Province, and the Daye Smelter, in Hubei province (Wu et al. 2011). A significant decrease in the heavy metal contents

Table 2 Total copper concentrations and contamination factors at the sampling points (no 30)

Sample no.	Geographic coordination		Depth = 0–10 cm		Depth = 10–30 cm		CCS (mg kg ⁻¹)
	Longitude (m)	Latitude (m)	SCC (mg kg ⁻¹)	CF	SCC (mg kg ⁻¹)	CF	
1	679,598	4,276,699	98.1	1.97	87.9	1.81	1698
2	679,590	4,276,677	257	5.19	154	3.17	1854
3	679,238	4,276,080	123	2.49	101	2.08	1659
4	679,080	4,275,710	101	2.05	87.2	1.79	1566
5	679,020	4,275,687	94.3	1.89	81.7	1.68	1248
6	678,486	4,574,631	87.2	1.75	71.2	1.46	1351
7	678,240	4,273,948	120	2.43	93.3	1.92	1116
8	678,318	4,273,550	72.6	1.46	74.5	1.53	982.7
9	678,248	4,273,193	87.1	1.75	62.4	1.28	1182
10	678,380	4,272,730	119	2.39	100	2.07	973.1
11	678,441	4,272,332	88.3	1.78	59.2	1.21	1148
12	678,497	4,272,188	155	3.12	82.7	1.69	1006
13	678,563	4,271,946	121	2.44	99.8	2.05	1140
14	678,558	4,271,790	102	2.07	81.4	1.67	1031
15	678,679	4,271,437	99.7	2.01	89.3	1.83	1033
16	678,778	4,270,918	73.5	1.48	76.2	1.56	792.3
17	678,606	4,270,814	90.1	1.81	71.2	1.46	964.8
18	678,435	4,270,667	72.9	1.47	83.7	1.72	1057
19	678,230	4,270,461	74.8	1.51	69	1.42	714.8
20	678,211	4,270,172	99.9	2.01	90.9	1.87	877.1
21	678,156	4,269,882	86.9	1.75	64.4	1.32	1034
22	678,285	4,269,552	80.9	1.63	74.9	1.54	971.1
23	678,265	4,269,307	94.9	1.91	88.5	1.82	1229
24	678,192	4,270,594	102	2.06	109	2.24	1221
25	678,334	4,268,143	121	2.44	80.9	1.66	998.4
26	678,330	4,267,954	114	2.31	87.7	1.8	444.4
27	678,381	4,267,200	92.4	1.86	74.8	1.53	1102
28	678,340	4,267,477	111	2.23	98.7	2.03	973.9
29	678,269	4,268,719	92.5	1.86	85.8	1.76	986.5
30	678,248	4,266,931	120	2.43	108	2.23	1118

SCC soil copper concentration, CF contamination factor, CCS copper concentration of surficial sediments

Table 3 Correlation coefficients between soil properties and SCC

Soil properties	OC	CCE	CEC	EC	pH	Clay	Sand	SCC
(Depth = 0–10 cm)								
OC	1							
CCE	0.149	1						
CEC	0.823**	-0.082	1					
EC	0.136	0.207	0.334	1				
pH	-0.624**	-0.068	-0.633**	0.498**	1			
Clay	0.007	0.029	0.439*	0.378*	0.285	1		
Sand	-0.222	-0.178	-0.611	-0.325	0.373	-0.734	1	
SCC	0.785**	-0.176	0.769**	0.086	-0.41*	0.181	-0.387*	1
(Depth = 10–30 cm)								
OC	1							
CCE	0.178	1						
CEC	0.543**	-0.212	1					
EC	0.577**	-0.363*	0.561**	1				
pH	-0.72**	0.252	-0.77**	-0.752**	1			
Clay	0.048	-0.095	0.502**	0.329	-0.381	1		
Sand	-0.19	-0.04	-0.811**	-0.277	0.552**	-0.607**	1	
SCC	0.737**	-0.134	0.493**	0.429*	-0.6**	0.113	-0.213	1

OC organic carbon, CCE calcium carbonate equivalent, CEC cation exchange capacity, EC electrical conductivity, pH soil reaction, SCC soil copper concentration

* $p < 5\%$; ** $p < 1\%$

Table 4 The best fitted models for semivariograms of the investigated soils at two depths and even surficial sediments using IDW² method

Soil properties	Depth (cm)	Model	C_o	C_o+C	A_o (m)	C_o/C_o+C (%)	R^2	RSS
Sand (%)	0–10	Spherical	111.8	225.4	4057	49.6	0.99	3.9
	10–30	Spherical	66.8	139.3	5049	48	0.99	0.87
Silt (%)	0–10	Spherical	66	85	3300	77.6	0.97	3.5
	10–30	Gaussian	69.1	255.7	4200	27	0.74	2.29
Clay (%)	0–10	Exponential	10^{-4}	0.16	411	10^{-4}	0.85	4.8×10^{-4}
	10–30	Spherical	0.01	28.01	1154	0	0.94	11.8
CCE (%)	0–10	Gaussian	0.37	1.07	10,110	34.4	0.61	3.4×10^{-3}
	10–30	Spherical	4.8	6.8	2300	70.6	0.71	0.61
pH	0–10	Spherical	0.01	0.07	21,100	21	0.81	1.9×10^{-4}
	10–30	Gaussian	0.01	0.23	11,670	5.1	0.98	10^{-5}
EC (dS m ⁻¹)	0–10	Spherical	4×10^{-3}	0.19	748	1.8	0.95	1.3×10^{-4}
	10–30	Gaussian	0.07	0.74	12,180	9.5	0.95	7.6×10^{-4}
OC (%)	0–10	Gaussian	4×10^{-3}	7×10^{-2}	15,980	5	0.93	1.4×10^{-5}
	10–30	Gaussian	6×10^{-4}	2×10^{-2}	17,180	4	0.95	2.7×10^{-7}
CEC (cmol _c kg ⁻¹)	0–10	Gaussian	0.03	0.25	11,630	10	0.94	3.9×10^{-4}
	10–30	Gaussian	14.2	78.4	6820	18	0.92	166
SCC (mg kg ⁻¹)	0–10	Gaussian	0.04	0.46	15,950	9	0.75	2.4×10^{-3}
	10–30	Spherical	0.02	0.06	6500	30	0.85	1.3×10^{-4}
CCS (mg kg ⁻¹)	–	Gaussian	0.03	0.75	16,030	4	0.97	6.7×10^{-4}

C_o nugget, c_o+c sill, A_o range parameter, CCE carbonate calcium equivalent, pH soil reaction, EC electrical conductivity, OC organic carbon, CEC cation exchange capacity, SCC soil copper concentration, CCS copper concentration of surficial sediments

from surface to depth of contaminated sites has been previously reported (Rodríguez-Tovar and Martín-Peinado 2014). Furthermore, there was a significant decrease in standard deviation values with increasing depth. This indicates that the contamination originated from an influx of surface-transported materials rather than a geological event.

Fairly good direct correlations were found between SCC and OC. Copper can form stable complexes with organic matter (Pandey et al. 2000). Positive correlations between copper concentration and dissolved organic matter were similarly found in the soil percolates of contaminated soils (Kalbitz and Wennrich 1998) and in the soil solutions of some agricultural lands (Romkens and Salomons 1998). The mobilization

of Cu and its uptake increased by rapeseed cultivation. Therefore, remediation via application of activated charcoal and phytoremediation using rapeseed may be recommended in the future investigations (Rinkelbe and Shaheen 2015). The results revealed a significant negative correlation between SCC and soil pH at two depths. However, the strength of relationship was higher in the subsurface soils than in the surface ones. The decrease in pH at high contaminated soils may be attributed to the copper hydrolysis. No significant correlation was found between the clay content and SCC in this research work. A positive correlation was found between SCC and EC of the soils at depth of 10–30 cm. This may be attributed to receiving and then leaching of soluble salts from

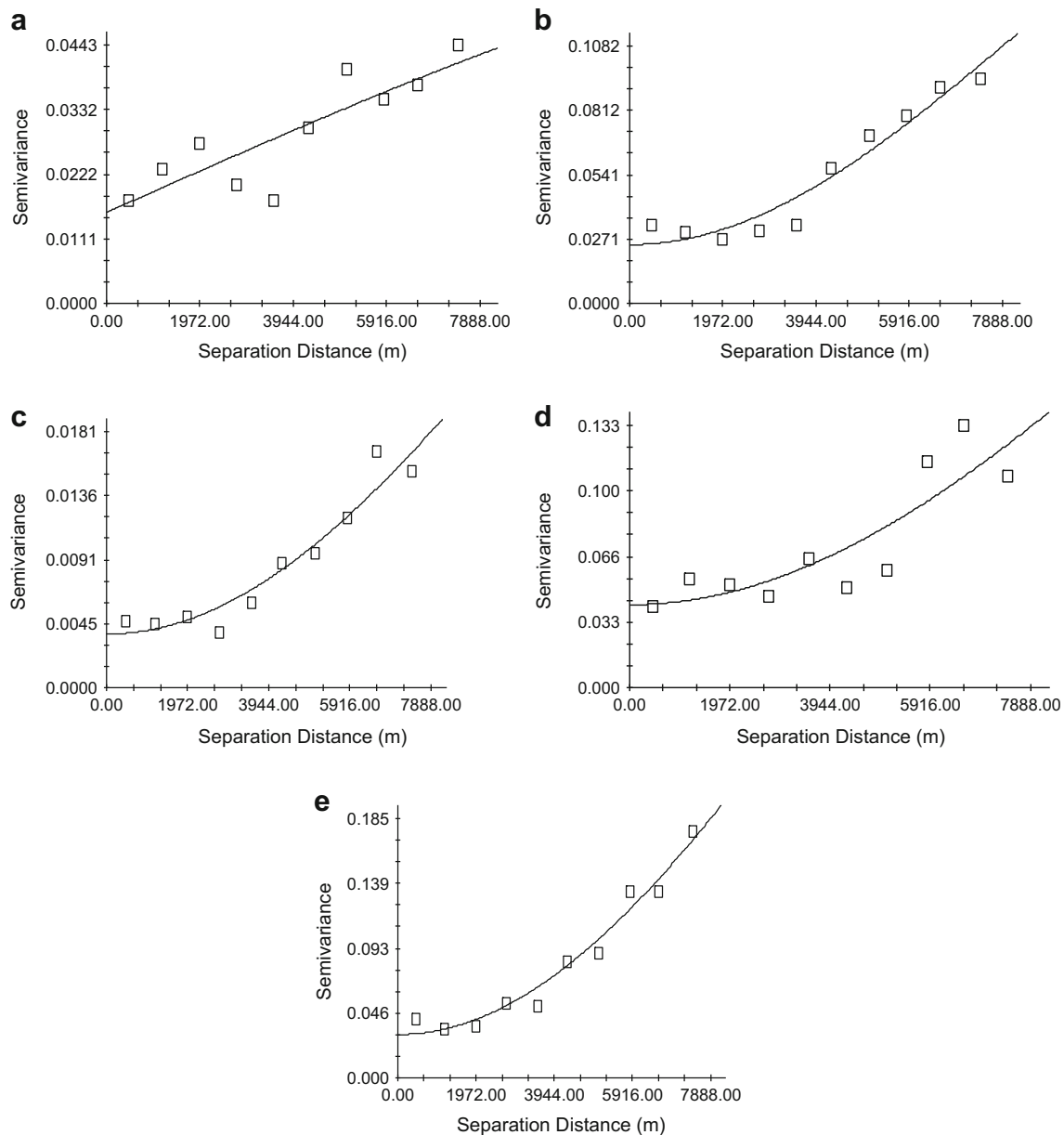


Fig. 2 The isotropic variogram models fitted to the selected soil surface properties. **a** Spherical model for pH. **b–d** Gaussian model for CEC, OC, and SCC. **e** CEC

transported materials. The SCC was also negatively correlated with sand content at depth of 0–10 cm. This may be due to low retention capacity of the coarse-textured upper horizons. The finding was in agreement with others (Usman 2008). The high correlation coefficient between SCC and CEC was a consequence of strong correlation between CEC and OC (Table 3).

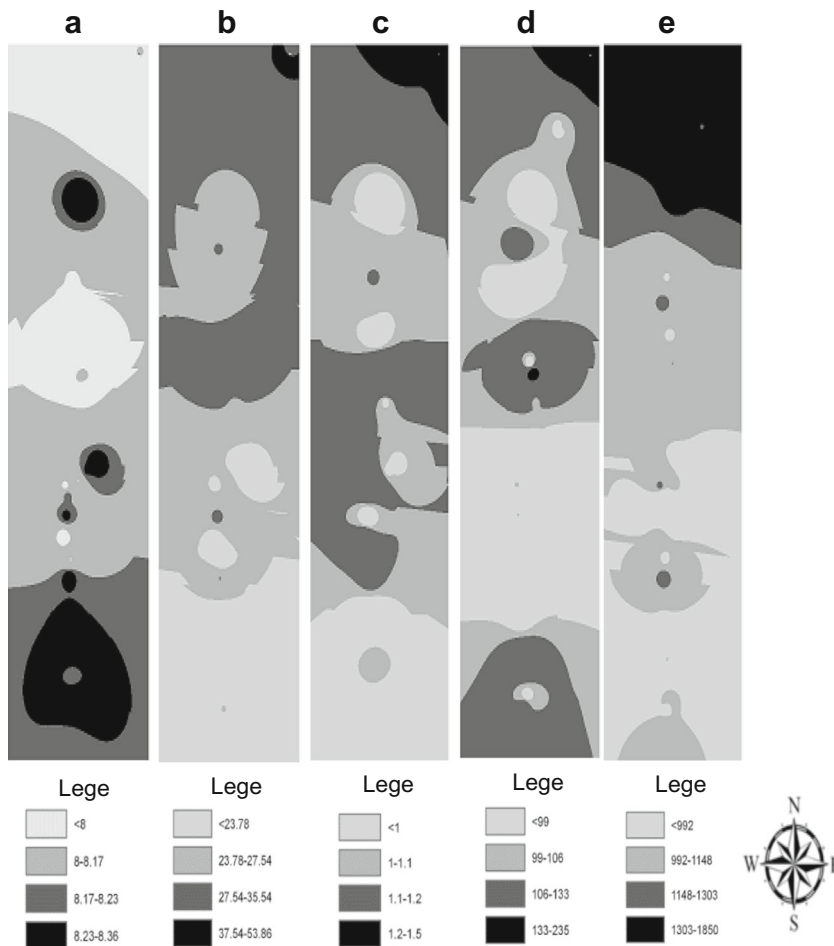
Moreover, results showed a significant positive correlation ($p < 0.01$) between SCC and the thickness of surficial materials in both depths. This is another reason confirming again that the source of copper contamination in the study soils is the tailings dam failure. The results also revealed that the mean value of CF in the surface soil samples near the tailings dam was about 14 which were very high. This is in consistent with findings of the previous reports (Veinott et al. 2003). There are several copper mines in the entire world (Chile, the USA, China, Morocco, etc.). The copper concentration in the tailings of the Dabaoshan (Shaoguan region, China), Jiuhuashan (Anhui province, China), and Anti-Atlas (Southern Morocco) mines were reported 1486, 1899, and 2527 mg kg⁻¹, respectively (Zhou et al. 2007). This concentration for the tailings dam materials in Mazraeh mine was 5870 mg kg⁻¹ which is approximately three times greater than the above-mentioned concentrations. This could be the consequence of low

recovery of copper from copper bearing ores. The mean value of CF for surface (0–10 cm) and subsurface soils (10–30 cm) was 2.1 and 1.77, respectively. This indicates the moderate contamination in the study area.

Geostatistical modelling and spatial variability

Spatial variability was investigated using semivariograms. The ratio of nugget to total semivariance, expressed as a percentage, was used to classify spatial dependence. A ratio of <25% indicated strong spatial dependence, between 25 and 75% indicated moderate spatial dependence, and >75% indicated weak spatial dependence (Cambardella et al. 1994). According to the best fitted models (considering higher R^2 and lower RSS) resulted from the geostatistical analyses, the ratio of nugget variance to the sill variance in surficial sediments was lower than soils. Additionally, this ratio for the upper 10 cm of the soils was lower than the next 20 cm. These results illustrated the more spatial dependence of copper distribution in sediments and upper 10-cm soils than in the next 20-cm soils. Either despite the high potential of soils to adsorb contaminants like Cu or these contaminants will all likely enter the surface and groundwater eventually

Fig. 3 Created maps of selected soil surface properties according to high accurate modelling. **a** pH. **b** CEC/ cmol_c kg⁻¹. **c** OC/ %. **d** SCC/ mg kg⁻¹. **e** CCS/ mg kg⁻¹



(Jahanshahi et al. 2014). Therefore, the probable transmission of copper into the lower depths or into the runoff must be considered in the design of the proposed dam. Derived parameters from geostatistical analysis are summarized for both soil depths and sediments in Table 4.

When data are limited, to predict successfully at unsampled points strongly depends on the relationships between accuracy, sample size, and sample spacing and to what extent these factors are related to the property under investigation (Schloeder et al. 2001). In order to interpolate some of

observed soil surface (0–10 cm) properties, the variogram models fitted to the experimental variograms are presented in (Fig. 2). The spherical model was appropriately fitted to interpolate pH variability (Fig. 2a). The similar results were previously reported (Silva et al. 2003). The exponential model was best fitted for interpolating soil clay content in the study area as well as it had been also found by others (Joshua et al. 2014). Moreover, the Gaussian model was also identified as a work horse modelling approach for interpolation the CEC, OC, SCC, and CCS (Fig. 2b–e).

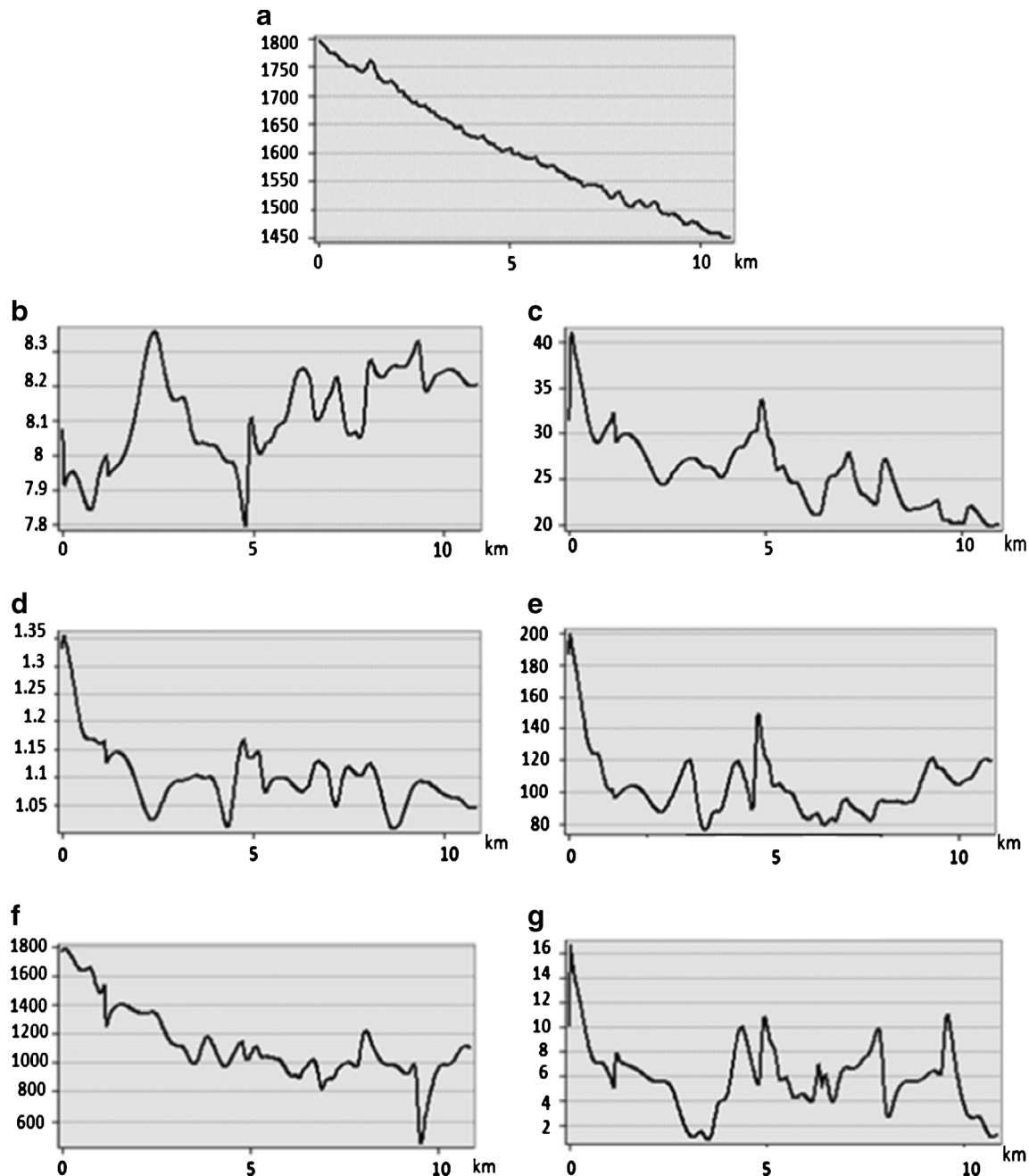


Fig. 4 Distance profile graphs of the selected soil surface properties. **a** DEM/ m. **b** pH. **c** CEC/ $\text{cmol}_c \text{ kg}^{-1}$. **d** OC/ %. **e** SCC/ mg kg^{-1} . **f** CCS/ mg kg^{-1} . **g** thickness of surficial sediments/ cm

Integrating modelling results with GIS

Digital mapping after selecting the most suitable modelling approach is the subsequent process to observe the spatiality distribution. As it appears from the results, the tailings dam has occurred in the north part of study area. The raster graphics of five surface properties were reclassified to four classes using the Geometrical Interval method (Fig. 3a–e). Spatial distribution and overlay analysis showed that the values of all parameters decreased from the north to the south part of area in the direction of flow. Major parts of the released materials with high copper concentration have been percolated in soils near the source and rest of them have been diluted by storm water along the direction flow. Obtained results from geostatistical analysis graphically represented in Fig. 3 are in agreement with the results of correlation analysis (Table 3) that were discussed above.

Unfortunately, lacks of precise terrain data and application experience are the most important limitations of applying terrain analysis in low relief areas (Gallant and Dowling 2003). Geostatistical methods cannot substitute conventional soil mapping; they can be an excellent aid for a better understanding of soil distribution. They allow us to consider the soil as a continuum; in this issue, they overcome conventional soil mapping (Wälder et al. 2008). As we know, the topographic profiles of each digital elevation model (DEM) represents the relationships between elevation and soil formation factors as well as processes. In fact, it shows the change in elevation of a surface along a line. Even a very gentle surface relief may exert deep influences on soil properties (McKenzie and Ryan 1999). Here, attention has been focused on the relationships between DEM and selected soil surface properties in the present study (Fig. 4). According to the obtained graphs, the general scheme of pH variations was vastly different compared to other parameters. When the pH was in peak at 2 km away from the source, CEC, OC, and SCC values were at the lowest level. On the contrary, reverse results were observed at 5 km away from the source. The distance profile graphs revealed that there are similarities on distribution patterns of the SCC and CCS in stream pathway from upper to lower part of the study area. Also, general scheme of graphs (Fig. 4e–g) shows that the thickness of surficial sediments in the direction of flow is corresponding to SCC and CCS.

References

- Adriano DC (2001) Trace elements in terrestrial environments: biogeochemistry, bioavailability, and risk of metals, 2nd edn. Springer-Verlag, New York
- Cambardella CA, Moorman TB, Parkin DL, Karlen JM, Novak R, Turco F, Konopka AE (1994) Field-scale variability of soil properties in central Iowa soils. *SSSAJ* 58:1501–1511
- Chapman HD (1965) Cation exchange capacity. In: Black CA et al. *Methods of soil analysis*, 2nd edn. Part 2, SSSA, Madison, WI, pp 891–901
- Chen M, Ma L (2001) Comparison of three aqua regia digestion methods for twenty Florida soils. *SSSAJ* 65:499–510
- Elliot P, Wakefield J, Best NJ, Briggs D (2000) *Spatial epidemiology methods and applications*, Oxford University Press
- Gallant JC, Dowling TD (2003) A multi-resolution index of valley bottom flatness for mapping depositional areas. *Water Resour Res* 39: 1347–1360
- Gee GW, Bauder HW (1986) Physical and mineralogical methods. In: Page AL (ed) *Methods of soil analysis*, 2nd edn. Part 1, SSSA, Madison, WI, pp 383–411
- Goovaerts P (1999) Geostatistics in soil science: state-of-the-art and perspectives. *Geoderma* 89:1–45
- Gotway CA, Ferguson RB, Hergert GW, Peterson TA (1996) Comparison of kriging and inverse distance methods for mapping soil parameters. *SSSAJ* 60:1237–1247
- Grzebisz W, Ciesla L, Diatta JB (2001) Spatial distribution of copper in arable soils and in non-consumable crops (flax, oil-seed rape) cultivated near a copper smelter. *Polish J Environ Stud* 10:269–273
- Hakanson L (1980) An ecological risk index for aquatic pollution control: a sedimentological approach. *Water Res* 14:975–1001
- Henderson BL, Webster R, McKenzie NJ (2008) Statistical analysis. In: McKenzie NJ, Grundy MJ, Webster R, Ringrose-Voase AJ (eds) *Guidelines for surveying soil and land resources*. CSIRO press, Australia, pp 327–348
- Hooker PJ, Nathaniel CP (2006) Risk-based characterization of lead in urban soils. *Chem Geol* 226:340–351
- Hutton M, Meeus C (2001) Analysis and conclusions from member states assessment of the risk to health and the environment from cadmium in fertilizers. Final report, European Commission-Enter-Prise DG; 1–134
- Jafarnejadi AR, Saadinejad S, Gholami A (2013) Spatial variation of copper in soils and grains of wheat farms in southern Iran. *Caspian J Appl Sci Res* 2:35–41
- Jahanshahi R, Zare M, Schneider M (2014) A metal sorption/desorption study to assess the potential efficiency of a tailings dam at the Golgohar iron ore mine, Iran. *Mine Water Environ* 33:228–240
- Joshua OO, Evelyn OO, Luis CT, Azubuike CO, Donald MJ (2014) Assessment of spatial distribution of selected soil properties using geospatial statistical tools. *Commun Soil Sci and Plant Anal* 45: 2182–2200
- Kabata-Pendias A (2011) *Trace elements in soils and plants*, 4rd edn. CRC Press, Boca Raton
- Kalbitz K, Wennrich R (1998) Mobilization of heavy metals and arsenic in polluted wetland soils and its dependence on dissolved organic matter. *Sci Total Environ* 209:27–39
- Khorasanipour M, Eslami A (2014) Hydro-geochemistry and contamination of trace elements in cu-porphyry mine tailings: a case study from the Sarcheshmeh mine, SE Iran. *Mine Water Environ* 33: 335–352
- Kravchenko A, Bullock DG (1999) A comparative study of interpolation methods for mapping soil properties. *SSSAJ* 91:391–400
- Lark RM, Ferguson RB (2004) Mapping risk of soil nutrient deficiency or excess by disjunctive and indicator kriging. *Geoderma* 118:39–53
- Leenaers H, Okx JP, Burrough PA (1990) Comparison of spatial prediction methods for mapping floodplain soil pollution. *Catena* 17:535–550
- Lu JY, Wong DW (2008) An adaptive inverse-distance weighting spatial interpolation technique. *Comput Geosci* 34:1044–1055
- McKenzie NJ, Ryan PJ (1999) Spatial prediction of soil properties using environmental correlation. *Geoderma* 89:67–94
- Nelson DW, Sommers LE (1982) Total carbon and organic matter. *Methods of Soil Analysis*, SSSA, Madison

- Pandey AK, Pandey SD, Misra V (2000) Stability constants of metal-humic acid complexes and its role in environmental detoxification. *Ecotoxicol Environ Safe* 47:195–200
- Rhoades JD (1996) Salinity: electrical conductivity and total dissolved solids. In: Sparks DL (ed) *Methods of soil analysis*. 3rd edn. Part 3, SSSA, Madison, WI, pp 417–435
- Rinkelbe J, Shaheen SM (2015) Miscellaneous additives can enhance plant uptake and affect geochemical fractions of copper in a heavily polluted riparian grassland soil. *Ecotoxicol Environ Safe* 119:58–65
- Rodríguez-Tovar FJ, Martín-Peinado FJ (2014) Lateral and vertical variations in contaminated sediments from the Tinto River area (Huelva, SW Spain): incidence on trace maker activity and implications of the palaeontological approach. *Palaeogeo, Palaeocli, Palaeoeco* 414:426–437
- Romkens PFAM, Salomons W (1998) Cd, Cu and Zn solubility in arable and forest soils: consequences of land use changes for metal mobility and risk assessment. *Soil Sci* 163:859–871
- Salomons W (1992) Environmental impact of metals derived from mining activities processes, predictions, and prevention. *J Geochem Explor* 52:5–23
- Schloeder CA, Zimmermann NE, Jacobs MJ (2001) Comparison of methods for interpolating soil properties using limited data. *SSSAJ* 65:470–479
- Shahbazi F, De la Rosa D (2010) Towards a new agriculture for the climate change era in West Asia, Iran. In: Simard SW, Austin ME (eds) *Climate change and variability*. SCIYO Publications, Croatia, pp 337–364
- Shahbazi F, Aliasgharzad N, Ebrahimzad SA, Najafi N (2013) Geostatistical analysis for predicting soil biological maps under different scenarios of land use. *Eur J Soil Bio* 55:20–27
- Silva VR, Reichert JM, Storck L, Feijo S (2003) Spatial variability of chemical soil properties and corn yield on a sandy loam. *Revista Brasileira de Ciência de Solo* 27:1013–1020 (in Spanish)
- Sun H, Juan L, Xiaojun M (2014) Heavy metals' spatial distribution characteristics in a copper mining area of Zhejiang province. *J Geog Info Sys* 4:46–54
- Thomas GW (1996) Soil pH and soil acidity. In: Sparks DL (ed) *Methods of soil analysis*. 3rdedn. Part 3, SSSA, Madison, WI, pp 475–490
- Tipper JC (2008) A simple method for representing some univariate frequency distributions, with particular application in Monte Carlo-based simulation. *Comput Geosci* 34:1154–1166
- USDA-NRCS (2004) *Soil survey laboratory methods manual*, Soil survey investigations report, No. 4, , Version 4, Washington, DC
- Usman A (2008) The relative sorption selectivity's of Pb, Cu, Zn, Cd and Ni by soils developed on shale in New Valley, Egypt. *Geoderma* 144:334–343
- Veinott G, Sylvester P, Hamoutene D, Anderson MR, Meade J, Payne J (2003) State of the marine environment at Little Bay Arm, Newfoundland and Labrador, Canada, 10 years after a “do nothing” response to a mine tailings spill. *J Environ Monit* 5:626–634
- Vrhovnik P, Dolenc T, Serafimovski T, Dolenc M, Smuc NR (2013) The occurrence of heavy metals and metalloids in surficial lake sediments before and after a tailings dam failure. *Polish J Environ Stud* 22:1525–1538
- Wälder K, Wälder O, Rinkelbe J, Menz J (2008) Estimation of soil properties with geostatistical methods in floodplains. *Arch Agron Soil Sci* 54:275–295
- Webster R (2001) Statistics to support soil research and their presentation. *Eur J of Soil Sci* 52:331–340
- Webster R (2008) *Geostatistics*. In: McKenzie NJ, Grundy MJ, Webster R, Ringrose-Voase AJ (eds) *Guidelines for surveying soil and land resources*. CSIRO press, Australia, pp 369–382
- Whelan BM, McBratney AB, Rossel RAV (1996) Spatial prediction for precision agriculture. In: *Proceedings of the 3rd International Conference on Precision Agriculture*, ASA/CSSA/SSSA, WI, USA
- Wu F, Liu YL, Xia Y, Shen ZG, Chen YH (2011) Copper contamination of soils and vegetables in the vicinity of Jiuhuashan copper mine, China. *Environ Earth Sci* 64:761–769
- Zhou JM, Dang Z, Cai MF, Liu CQ (2007) Soil heavy metal pollution around the Dabaoshan mine, Guangdong province, China. *Pedosphere* 17:588–594